

The formation of multiple populations in the globular cluster 47 Tuc

P. Ventura^{1*}, M. Di Criscienzo², F. D’Antona¹, E. Vesperini⁵, M. Tailo^{1,3},
F. Dell’Agli^{1,3}, A. D’Ercole⁴

¹*INAF-Osservatorio Astronomico di Roma, Via Frascati 33, Monte Porzio Catone 00040, Italy*

²*INAF-Osservatorio Astronomico di Capodimonte, Salita Moiariello 16, Napoli 80131, Italy*

³*Dipartimento di Fisica, Università di Roma “La Sapienza”, Italy*

⁴*INAF-Osservatorio Astronomico di Bologna, Via Ranzani 1, Bologna 40127, Italy*

⁵*Department of Astronomy, Indiana University, Bloomington, USA*

Accepted, Received; in original form

ABSTRACT

We use the combination of photometric and spectroscopic data of 47 Tuc stars to reconstruct the possible formation of a second generation of stars in the central regions of the cluster, from matter ejected from massive Asymptotic Giant Branch stars, diluted with pristine gas.

The yields from massive AGB stars with the appropriate metallicity ($Z=0.004$, i.e. $[\text{Fe}/\text{H}]=-0.75$) are compatible with the observations, in terms of extension and slope of the patterns observed, involving oxygen, nitrogen, sodium and aluminium.

Based on the constraints on the maximum helium of 47 Tuc stars provided by photometric investigations, and on the helium content of the ejecta, we estimate that the gas out of which second generation stars formed was composed of about one-third of gas from intermediate mass stars, with $M \geq 5M_{\odot}$ and about two-thirds of pristine gas. We tentatively identify the few stars whose Na, Al and O abundances resemble the undiluted AGB yields with the small fraction of 47 Tuc stars populating the faint subgiant branch.

From the relative fraction of first and second generation stars currently observed, we estimate that the initial FG population in 47 Tuc was about 7.5 times more massive than the cluster current total mass.

Key words: Stars: abundances – Stars: AGB and post-AGB – Globular clusters: general

1 INTRODUCTION

The traditional paradigm that stars in Globular Clusters (GC) are an example of a coeval and chemically homogeneous population was challenged by photometric and spectroscopic results, which highlighted the presence of at least two generations of stars: a first generation (FG), with the chemistry of the cloud from which the cluster formed, and an additional component (second generation, hereinafter SG), with a composition showing the signature of proton-capture nucleosynthesis.

The surface abundances of stars belonging to the SG define abundance patterns, where sodium is correlated to aluminium, and anticorrelated to magnesium and oxygen. The extension and the slope of these trends change from

cluster to cluster, but it is interesting that they have been detected within each GC investigated so far (Gratton et al. 2004, 2012). These chemical anomalies involve only “light” elements, up to silicon, whereas no spread is observed in the iron content¹.

On the photometric side, the hypothesis that the morphology of the Horizontal Branch (HB) of some GCs could be explained by the presence of two or more populations, differing in their original content of helium, came from the seminal paper by D’Antona et al. (2002), and subsequently extended to NGC 2808 (D’Antona & Caloi

¹ There are indeed a few clusters in which an iron variation is present, such as ω Cen (e.g. Norris et al. 1996) and M 22 (e.g. Marino et al. 2009). Their chemical evolution must have been more complex than in standard mono-metallic clusters.

* E-mail: paolo.ventura@oa-roma.inaf.it (AVR)

2004), M3 and M13 (Caloi & D’Antona 2005), NGC 6441 (Caloi & D’Antona 2007).

These early speculations were later confirmed by detailed photometric analysis of the Main Sequence (MS) of the cluster NGC 2808, which was shown to be split in three components, differing in their helium content (D’Antona et al. 2005; Piotto et al. 2007). Subsequent investigations detected a splitting in the MS of NGC 6752 (Milone et al. 2010), and in the subgiant branches (SGBs) of NGC 1851, NGC 6656, 47 Tuc, and other five GCs (Milone et al. 2008; Marino et al. 2009; Anderson et al. 2009; Piotto et al. 2012).

This impressive set of evidence indicates that in most (if not all) GCs a self-enrichment mechanism must have produced gas contaminated by p-capture nucleosynthesis, such that one or more additional generations of stars formed, and are currently co-existing with the original population.

According to the most complete scenario suggested so far, a crucial role as polluters of the intra-cluster medium was played by stars of intermediate mass during the Asymptotic Giant Branch (AGB) phase (Ventura et al. 2001). The paper by D’Ercole et al. (2008) set the theoretical framework to describe the formation of SG stars in GCs, by gas ejected by AGBs possibly mixed with pristine gas, survived to the epoch of supernovae explosions. This approach allowed to reconstruct the formation of multiple populations in M4 (an example of a cluster showing mild anomalies) and NGC 2808 (example of a cluster hosting, in addition, an extremely helium rich population) (D’Ercole et al. 2010, 2012).

As we will show in this paper to reproduce the observed abundance patterns processed gas provided only by AGB stars with masses between about $5M_{\odot}$ and $8M_{\odot}$ can be used along with some pristine gas. As already discussed in several of the papers cited above, the amount of gas available for SG formation in this scenario (as well in other competing scenarios for which a detailed study of the resulting abundance patterns have been investigated; see e.g. Bekki et al. (2007); D’Ercole et al. (2008); Decressin et al. (2007); Renzini (2008); Carretta et al. (2009); Bekki (2011)) implies that the FG cluster must have initially been more massive. We discuss the specific implications of the model presented here in section 4.

The globular cluster NGC 104, better known as 47 Tuc, is a valuable test to understand the formation process of multiple populations in globular clusters. Until a few years ago it was considered as the prototype of a single stellar population, based on the photometric morphology of the MS and the HB. The first challenge to this belief came from the analysis based on the HST archival data by Anderson et al. (2009), showing the splitting of the SGB in two components, separated in magnitude. Di Criscienzo et al. (2010) then showed that the morphology of the HB of 47 Tuc is consistent with the presence of two populations, differing in helium content up to a maximum of $\Delta Y \sim 0.03$. Such interpretation was recently confirmed by the detailed photometric analysis published in Milone et al. (2012a), who explained the complex of the observed colours of MS stars with a couple of populations, one with the primeval composition, and another with a small helium enhancement, which, in agreement with Di Criscienzo et al. (2010), is within $\Delta Y = 0.03$.

From a spectroscopic point of view, a bimodal distri-

bution of CN band strengths among giant stars belonging to 47 Tuc was found by Briley (1997). The following analyses by Cannon et al. (1998) and Harbeck et al. (2003), showed that this bimodality still exists 2.5 mag below the Turn Off, suggesting the presence of two populations in the cluster, differing in their chemistry. The presence of a O–Na anticorrelation in unevolved stars was first detected by Carretta et al. (2004), based on the spectroscopic analysis of 7 objects, confirmed by Carretta et al. (2009) and by D’Orazi et al. (2010), who investigated a much more complete sample, made of 109 sources. A step forward was made by Gratton et al. (2013), who found a correlation among the color of HB stars and the abundances of oxygen, sodium and aluminium, and by Carretta et al. (2013), who presented the chemical patterns defined by 116 giants in 47 Tuc.

This rich set of data allows one to test whether the self-enrichment mechanism by AGBs can explain the patterns traced by stars in 47 Tuc, and account for the distribution of HB and MS stars in the Color–Magnitude diagram. For this purpose, we calculated a set of AGB models having an input chemistry appropriate for stars in this cluster, we determined the composition of the ejecta, and tested whether the observed patterns’ extension and slope are reproduced. We use work by Di Criscienzo et al. (2010) and Milone et al. (2012a) to determine the dilution with pristine material needed to allow the maximum spread of helium detected: this will set a limit to the most extreme chemistry that can be obtained.

2 THE STELLAR MODELS

2.1 Numerical and physical inputs

The evolutionary sequences used in the present investigation were calculated by means of the ATON code for stellar evolution. The interested reader may find in Ventura et al. (1998) a detailed description of the code. The micro- and macro-physics adopted are the same as in the recent investigations by our group on this topic, and can be found, e.g., in Ventura & D’Antona (2009).

In regions unstable to convective motions, the temperature gradient is found via the Full Spectrum of Turbulence (hereinafter FST) model (Canuto & Mazzitelli 1991). Mixing of chemicals is coupled to nuclear burning via a diffusive approach, using the schematization by Cloutmann & Eoill (1976). The overshoot of convective bubbles into radiatively stable regions is described by an exponential decay of convective velocities, characterized by an e-folding distance proportional to the parameter ζ . For all the evolutionary phases preceding the AGB phase we chose $\zeta = 0.02$, in agreement with our previous explorations, based on the calibration given in Ventura et al. (1998). For the AGB evolution, we calibrated the possible extra-mixing from the base of the convective envelope and from the borders of the convective shell which forms following the ignition of thermal pulses in order to reproduce the luminosity function of carbon stars in the Large Magellanic Cloud. By following this approach, similar to Marigo & Girardi (2007), we find $\zeta = 0.002$.

The range of masses involved is $1M_{\odot} \leq M \leq 8M_{\odot}$. Models of smaller mass hardly experience the AGB phase, and are however not of interest for the scope of this paper.

Stars of mass exceeding $8M_{\odot}$ are expected to undergo core-collapse, thus skipping the AGB phase. For each mass we followed the evolution from the pre-main sequence up to the almost complete loss of the convective envelope. Models of mass below $2M_{\odot}$ experience the helium flash at the tip of their red giant phase. The evolutionary sequences for these masses were re-started from the horizontal branch, where He-burning takes place in the non degenerate core resulting from the flash.

Stars of mass above $6.5M_{\odot}$ undergo carbon ignition in a degenerate layer above the core: these models develop a core made up of oxygen and neon, and experience a series of thermal pulses, as their lower mass counterparts (Garcia Berro et al. 1997; Ritossa et al. 1996, 1999; Siess 2006, 2007, 2010).

The initial composition in terms of metal and helium abundance is $Z=0.004$ and $Y=0.26$. This chemistry is similar to the models presented in Ventura & D’Antona (2008a), based on the mass fractions of the individual species given by Grevesse & Sauval (1998); the difference is that in the present investigation the mixture is assumed to be alpha-enhanced, with $[\alpha/\text{Fe}]=+0.2$ (in Ventura & D’Antona (2008a) we used $[\alpha/\text{Fe}]=+0.4$). These choices, assuming a solar metallicity $Z_{\odot} = 0.017$, correspond to an iron content $[\text{Fe}/\text{H}] = -0.75$, the same measured in 47 Tuc stars (Carretta et al. 2009). In addition to Ventura & D’Antona (2008a) paper we calculated the SAGB evolution of stars with mass $M > 6.5M_{\odot}$.

2.2 AGB evolution and stellar yields

Following the pioneering investigations by Schwarzschild & Harm (1965, 1967), we know that stars of intermediate mass, after the end of core helium burning, experience a series of thermal pulses (TPs), in the evolutionary phase known as Asymptotic Giant Branch. An updated, exhaustive description of the main features of the AGB evolution can be found, e.g., in Herwig (2005) and Karakas (2011).

The composition of the gas ejected by AGBs depends on the interface between the two mechanisms able to alter the surface chemistry: a) Third Dredge-Up (TDU), i.e. the inwards penetration of the convective envelope down to layers previously touched by 3α activity, and b) Hot Bottom Burning (HBB), with the activation of p-capture nucleosynthesis at the bottom of the surface convective layer (Renzini & Voli 1981; Blöcker & Schönberner 1991). TDU favours the increase of the surface carbon, and is the dominant mechanism in low-mass AGBs, with $M \leq 3M_{\odot}$. More massive stars may experience HBB, provided that the temperature at the base of their envelope exceeds $\sim 40\text{MK}$.

The efficiency of both mechanisms is unfortunately sensitive to the macro-physics description used. The extent of TDU depends on the treatment of convective borders, particularly to the extra-mixing from the base of the convective envelope and the boundaries of the convective shell which forms after each TP.

The strength of HBB is extremely sensitive to the convective model adopted (Ventura & D’Antona 2005). Models calculated with the Full Spectrum of Turbulence description of the convective regions are found to experience a much stronger HBB in comparisons with models of same mass

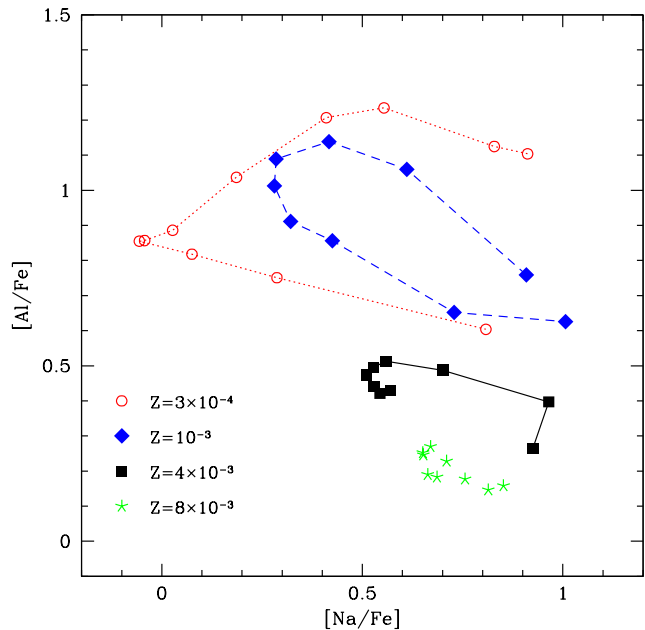


Figure 2. Sodium and Aluminium abundances of the gas expelled by AGB stars in the $[\text{Na}/\text{Fe}]$ – $[\text{Al}/\text{Fe}]$ plane. The results presented in this work, connected with a solid line, are indicated with full, black squares. The other points indicate results for different metallicities published in Ventura et al. (2013). For the sake of clarity, we only show yields for masses experiencing HBB, with $M \geq 4M_{\odot}$. For each metallicity, results for increasing mass are in the counter-clockwise direction.

and metallicity calculated by means of the traditional Mixing Length Theory of turbulent convection.

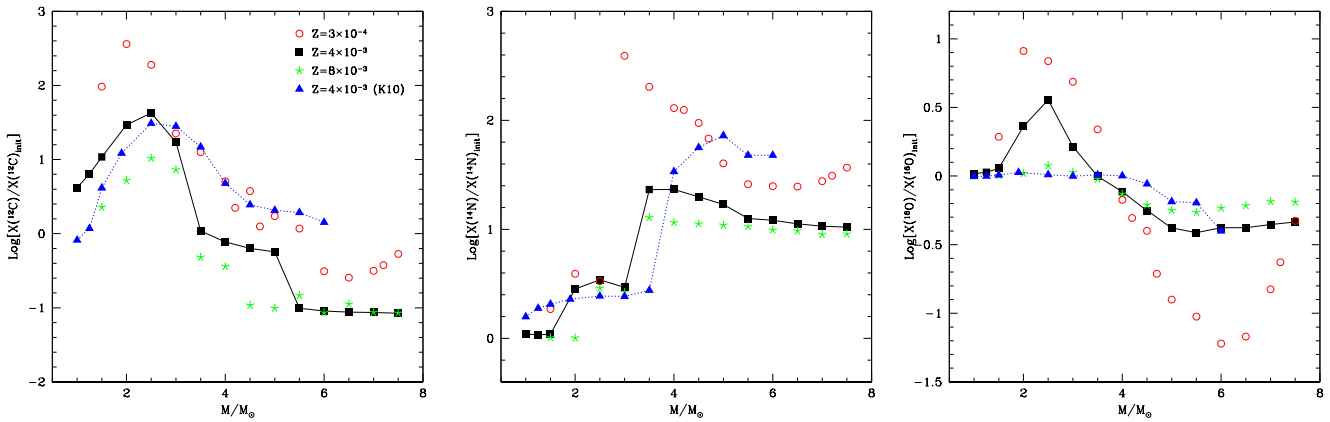
Table 1 summarizes the main physical and chemical results for the models investigated. For each mass we show the evolutionary time scale, the core mass at the beginning of the AGB phase, the maximum temperature achieved at the bottom of the convective envelope, and the average composition of the ejecta. For the i -th element we indicate the quantity $[i/\text{Fe}] = \log(X_i/X(\text{Fe})) - \log(X_i/X(\text{Fe}))_{\odot}$. For helium and lithium we show, respectively, the average mass fraction in the ejecta (Y), and the quantity $\log(\epsilon(\text{Li})) = \log(n(\text{Li})/n(\text{H})) + 12$.

Col. 5 of Table 1 shows that the ejecta of AGBs are helium-rich, as a consequence of the two dredge-up episodes following the core H- and He-burning phases, and, for the models experiencing HBB, of the p-capture nucleosynthesis at the bottom of the surface convective layer. Models with mass exceeding $5M_{\odot}$ produce ejecta with a helium mass fraction $Y \sim 0.35$, almost 0.1 larger than the initial abundance. This prediction, unlike those regarding the other species, is rather robust, because most of the helium enrichment occurs during the second dredge-up, which makes this finding independent of the uncertainties affecting the following thermal pulses phase (Ventura 2009).

The three panels of Fig. 1 show the average content of the gas ejected as a function of the initial mass, in terms of the mass fractions of carbon (left panel), nitrogen (middle) and oxygen (right). To better understand the extent of the variation from the initial content of each species, we show the ratio between the average and the initial abundance.

Table 1. Relevant properties of $Z = 4 \times 10^{-3}$ AGB and SAGB models

| M/M_{\odot} | τ_{evol} | M_c/M_{\odot} | $T_{\text{bce}}^{\text{max}}$ | Y | Li | [C/Fe] | [N/Fe] | [O/Fe] | [Na/Fe] | [Mg/Fe] | [Al/Fe] |
|---------------|----------------------|-----------------|-------------------------------|-------|-------|--------|--------|--------|---------|---------|---------|
| 1.0 | 6.4e9 | 0.53 | 2.4e6 | 0.283 | -1.66 | 0.62 | 0.04 | 0.22 | 0.02 | 0.20 | 0.00 |
| 1.25 | 3.1e9 | 0.54 | 3.1e6 | 0.284 | -1.93 | 0.81 | 0.03 | 0.23 | 0.04 | 0.20 | 0.00 |
| 1.5 | 2.0e9 | 0.55 | 3.8e6 | 0.287 | -1.90 | 1.04 | 0.04 | 0.26 | 0.08 | 0.20 | 0.00 |
| 2.0 | 1.1e9 | 0.50 | 4.1e6 | 0.270 | 1.49 | 1.47 | 0.45 | 0.56 | 0.43 | 0.25 | 0.20 |
| 2.5 | 5.7e8 | 0.57 | 5.5e6 | 0.296 | 1.40 | 1.63 | 0.54 | 0.76 | 0.64 | 0.47 | 0.73 |
| 3.0 | 3.4e8 | 0.70 | 2.3e7 | 0.283 | 1.90 | 1.24 | 0.47 | 0.42 | 0.33 | 0.31 | 0.55 |
| 3.5 | 2.3e8 | 0.79 | 8.1e7 | 0.283 | 2.80 | 0.04 | 1.37 | 0.19 | 1.01 | 0.22 | 0.20 |
| 4.0 | 1.7e8 | 0.82 | 8.7e7 | 0.304 | 2.34 | -0.11 | 1.37 | 0.08 | 0.93 | 0.21 | 0.27 |
| 4.5 | 1.3e8 | 0.85 | 9.2e7 | 0.324 | 2.42 | -0.20 | 1.30 | -0.06 | 0.97 | 0.20 | 0.40 |
| 5.0 | 1.0e8 | 0.89 | 9.6e7 | 0.339 | 2.33 | -0.24 | 1.23 | -0.13 | 0.70 | 0.18 | 0.49 |
| 5.5 | 8.4e7 | 0.96 | 1.01e8 | 0.347 | 2.35 | -1.00 | 1.01 | -0.18 | 0.57 | 0.17 | 0.52 |
| 6.0 | 6.7e7 | 1.01 | 1.05e8 | 0.357 | 2.44 | -1.04 | 1.08 | -0.19 | 0.54 | 0.17 | 0.50 |
| 6.5 | 5.9e7 | 1.07 | 1.07e8 | 0.356 | 2.45 | -1.06 | 1.05 | -0.18 | 0.52 | 0.16 | 0.48 |
| 7.0 | 5.1e7 | 1.18 | 1.11e8 | 0.361 | 2.49 | -1.06 | 1.03 | -0.15 | 0.53 | 0.16 | 0.46 |
| 7.5 | 4.4e7 | 1.27 | 1.14e8 | 0.367 | 2.74 | -1.07 | 1.02 | -0.13 | 0.54 | 0.17 | 0.44 |
| 8.0 | 4.0e7 | 1.33 | 1.24e8 | 0.375 | 3.24 | -1.05 | 1.01 | -0.12 | 0.57 | 0.17 | 0.43 |

**Figure 1.** The average mass fractions of carbon (Left), Nitrogen (middle) and Oxygen (Right) in the ejecta of AGB and SAGB stars, as a function of the initial mass. The ordinate shows the ratio of the abundance of the elements to the initial mass fraction. The results presented here, with metallicity $Z=0.004$, are indicated with black, full squares, and are connected with solid lines. The blue triangles indicate the results by K10, and are connected with a dotted curve. Red, open points and green asterisks show, respectively, results for metallicities $Z = 3 \times 10^{-4}$ and $Z = 8 \times 10^{-3}$ by Ventura et al. (2013).

The present results are compared with previous findings for different metallicities published in Ventura et al. (2013), and with models of the same metallicity by Karakas (2010) (hereinafter K10).

Both the present models and those by K10 show an increase in the carbon content of the ejecta in the low-mass domain, for $M \leq 3M_{\odot}$: this is due to the repeated TDU episodes, that transport to the stellar surface carbon synthesized in the 3α burning shell. The trend of $X(^{12}\text{C})$ with mass is rather similar in the two cases, as also the maximum increase in the carbon content, found to be $\delta(\text{C}) \sim 1.5 - 1.6$ dex. The results between this investigation and the work by K10 are different for $M \geq 3.5M_{\odot}$, because our models experience a stronger HBB, with a faster destruction of the surface carbon: while the yields by K10 are enriched in carbon for all masses, our models experiencing HBB show a carbon decrease, which reaches the asymptotic value of $\delta(\text{C}) \sim -1$ dex in the SAGB domain.

The different extent of the HBB experienced is also the

reason for the difference in the oxygen content of the ejecta (see right panel) for $M \geq 3.5M_{\odot}$: in the present compilation the oxygen is systematically lower than in K10, with the only exception of the $6M_{\odot}$ model, which shows the same depletion of $\delta(\text{O}) \sim -0.4$ dex in the two cases.

The trend of the nitrogen abundance with mass shows an abrupt increase around $\sim 3M_{\odot}$, because in that range of mass the carbon dredged-up to the surface is converted into nitrogen during the following interpulse phase. Note that in the $M \geq 3.5M_{\odot}$ domain our nitrogen yields are lower than K10, because the stronger HBB experienced by our models limits the number of thermal pulses, and thus the amount of carbon available.

An important consequence of the strong HBB in the envelope of massive AGB models calculated with the FST description of convection is that TDU is scarcely efficient in modifying the surface chemistry: as discussed previously, the star loses the whole envelope after a limited number of TPs, before TDU becomes efficient (Ventura & D'Antona 2008b).

This, in turn, implies that the overall C+N+O content of the ejecta of massive AGBs (with $M > 5M_{\odot}$) and SAGBs is practically unchanged with respect to the initial abundance, as expected from a pure p-capture nucleosynthesis (Ventura & D’Antona 2009).

The differences between models with different chemistry are due to the different impact of TDU and HBB in models with different metallicities. In the low mass domain, where the yields are dominated by TDU, the percentage increase in the surface carbon is larger for models with lower Z , because the same amount of carbon transported to the surface produces a larger increase in the surface abundance. The lower metallicity models experience a stronger HBB (Ventura et al. 2013): this is the reason why models with $Z = 3 \times 10^{-4}$ have a much smaller oxygen content than their higher Z counterparts. The opposite behaviour is found in the $Z = 8 \times 10^{-3}$ case, where only a modest depletion of the surface oxygen is achieved.

We note in the right panel of Fig. 1 that in the range of massive AGBs and SAGBs the low- Z models are characterized by a broad range of oxygen, while the models with $Z = 4 \times 10^{-3}$ (and even more those with $Z = 8 \times 10^{-3}$) have a much smaller variation of oxygen with mass. The reason for this difference is, again, the stronger HBB experienced by massive AGBs of smaller metallicity: the fast increase in the surface luminosity favours a large increase in the mass loss rate, such that in the models with the largest core masses the envelope is lost rapidly, before an advanced nucleosynthesis can be achieved. The trend of the oxygen content of the ejecta with mass is consequently not monotonic, the SAGB models showing up traces of a milder nuclear processing (Ventura & D’Antona 2011).

In Fig. 2 we show the sodium and aluminium content of the ejecta of the models presented here, compared to models of different metallicities published in Ventura et al. (2013). In the $[\text{Na}/\text{Fe}]$ - $[\text{Al}/\text{Fe}]$ plane we only show the yields of masses experiencing HBB, with $M \geq 4M_{\odot}$.

The interpretation of the aluminium abundances is straightforward. Lower metallicity models undergo stronger HBB, thus the Mg-Al nucleosynthesis proceeds faster. This can be clearly seen in the right panel of Fig. 3, showing the variation of the surface Al abundance in models of various mass and metallicity. The increase of Al with respect to the initial abundance is enhanced in low- Z models, whereas it is extremely small in the $Z = 8 \times 10^{-3}$ case. In the $Z = 3 \times 10^{-4}$ models (and also in the $Z = 10^{-3}$ ones, not shown here for clarity reasons) the temperatures at the bottom of the surface convective zone become so large that eventually an equilibrium stage is reached, such that the rates of production and destruction of Aluminium balance each other (Ventura et al. 2011): this is the motivation of the counter-clockwise shape of the $[\text{Na}/\text{Fe}]$ - $[\text{Al}/\text{Fe}]$ trends in Fig. 2 for these two metallicities, with the largest masses showing a smaller Al-enhancement in their ejecta.

In the $Z = 4 \times 10^{-3}$ models presented here the temperature at the bottom of the convective envelope hardly exceeds 10^8 K (see col. 4 of Table 1), thus the Al-burning channel is never activated: the behaviour of the various masses involved is much more homogeneous (see right panel of Fig. 3), and the extent of the increase in Al in the ejecta is approximately independent of mass, for $M \geq 5M_{\odot}$: for the present mixture,

massive AGBs produce winds with an average increase in the Aluminium content of $\delta[\text{Al}/\text{Fe}] \sim +0.5$ dex.

The behaviour of sodium is more tricky, given the different sensitivity to temperature of the production and destruction channels (Ventura & D’Antona 2006). While for temperatures below $\sim 70\text{MK}$ sodium is produced at the expense of neon, for larger T ’s the destruction process takes over. The typical behaviour of the surface sodium during the AGB evolution (see left panel of Fig. 3) shows an initial increase, followed by a depletion of the surface abundance in the latest evolutionary phases.

The higher is the temperature, the strongest is the rate at which sodium is consumed: lower metallicity models show on the average a lower content of sodium in the ejecta, as shown in Fig. 2. In low Z , SAGB models, mass loss is so fast to prevent a great destruction of the surface sodium (Ventura & D’Antona 2011): this is the reason for the large sodium content in the ejecta of the most massive models of $Z = 3 \times 10^{-4}$ and $Z = 10^{-3}$.

At $Z = 4 \times 10^{-3}$ sodium is initially produced in massive AGBs, the surface abundance increasing by almost a factor ~ 10 compared to the initial mass fraction. Unlike their lower Z counterparts, the destruction process proceeds later at a very slow pace. The sodium content of the ejecta is not very sensitive to the initial mass: we find that the sodium increase in the gas lost is $\delta[\text{Na}/\text{Fe}] \sim +0.5$ dex.

To summarize our findings, we conclude that massive AGBs with the chemistry examined here suffer a mild HBB. The gas ejected by these stars is expected to present the signature of p-capture burning, with the depletion of the surface content of oxygen of -0.4 dex, and an enhancement of the surface sodium and aluminium of $+0.5$ dex. The nucleosynthesis experienced is not sufficiently advanced to produce any modification of the surface silicon, whereas the overall content of magnesium is poorly reduced with respect to the initial abundance, of ~ 0.04 dex². The gas ejected is helium-rich, with an average helium of $Y \sim 0.35$. Finally, for what concerns the overall content of CNO, the yields from models with mass above $5M_{\odot}$ are found to maintain the initial C+N+O, whereas for $4M_{\odot} \leq M \leq 5M_{\odot}$ the increase in the total CNO ranges from 20% up to almost $\sim 100\%$.

3 THE INTERPRETATION OF THE CHEMICAL PATTERNS TRACED BY 47 TUC STARS

The recent investigation by Carretta et al. (2013) shows that stars in 47 Tuc trace well defined abundance patterns, involving some of the elements touched by p-capture nucleosynthesis. Sodium is correlated to aluminium and to nitrogen, and anticorrelated to oxygen. The present data do not allow to confirm possible variations in the abundances of magnesium and silicon, but the variation of these elements, if present, cannot exceed a few percent.

In the O-Na plane similar trends were found by the

² The overall magnesium content is only modestly touched by the nucleosynthesis experienced. However, the internal distribution among the Mg isotopes is considerably different in comparison with the initial mixture: most of the ^{24}Mg is lost, whereas ^{25}Mg is increased by almost one order of magnitude.

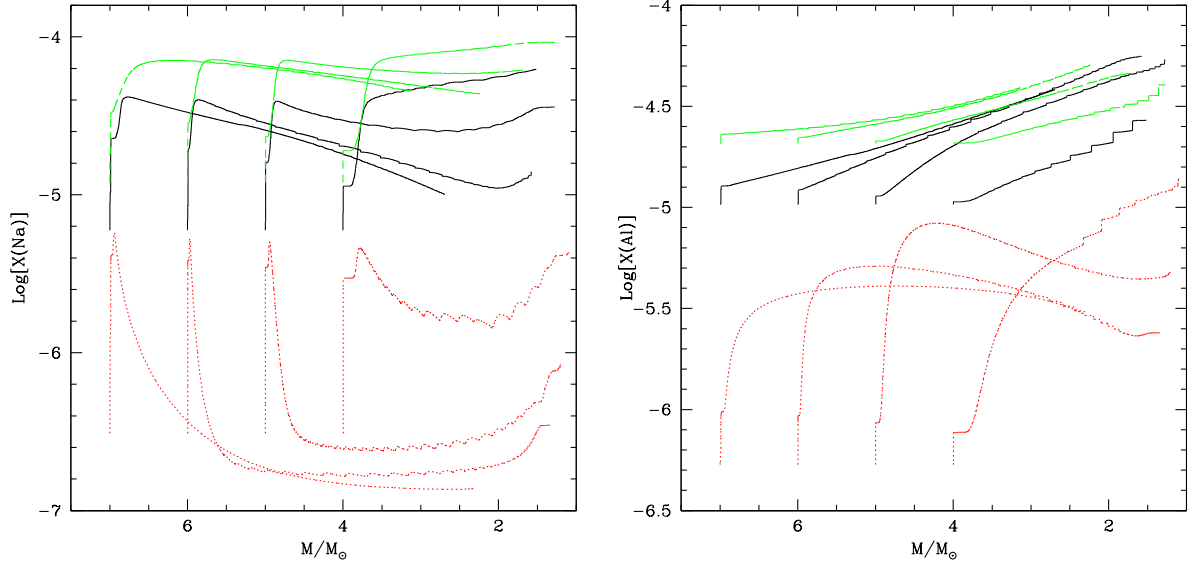


Figure 3. The variation during the AGB phase of the surface abundances of sodium (Left) and Aluminium (Right) in AGB models of initial mass 4,5,6,7 M_{\odot} and various metallicities. The total mass of the star (decreasing during the evolution) is reported on the abscissa. The models discussed in this work are indicated with full, black lines. Red, dotted curves indicate the results for $Z=3 \times 10^{-4}$, whereas green, dashed lines refer to $Z=8 \times 10^{-3}$ models.

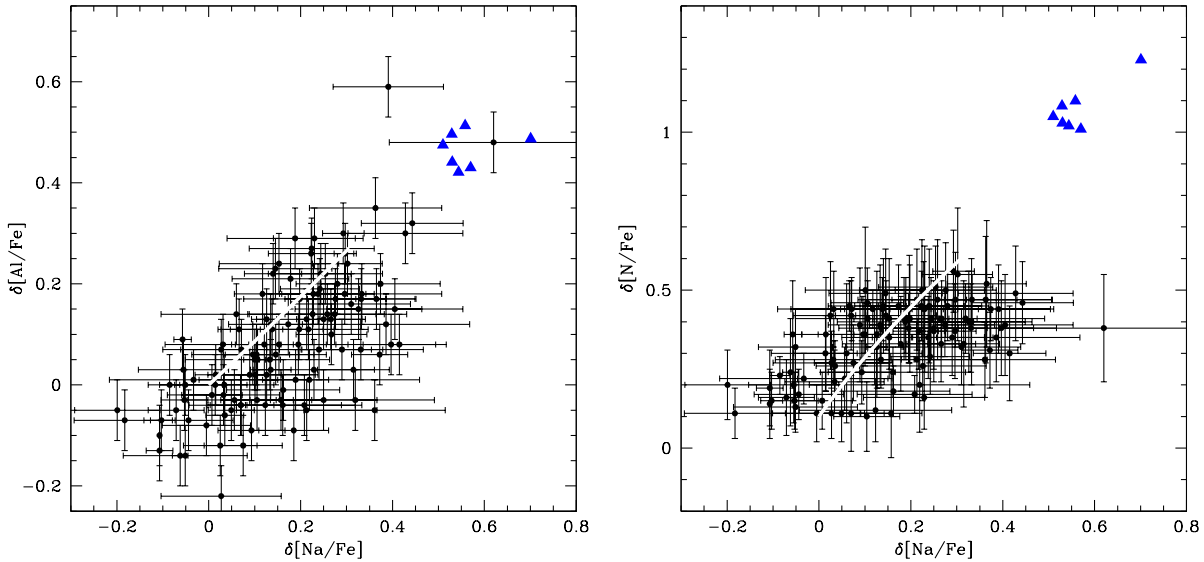


Figure 4. Left: Sodium and aluminium abundances observed in 47 Tuc stars by Carretta et al. (2013) (black points) and in the ejecta of massive AGB and SAGB stars presented in Table 1 (blue, full triangles). Only models with $M \geq 5M_{\odot}$ are shown. The observed abundances of sodium and aluminium were shifted, respectively, by -0.3 and -0.45 dex, to account for the offset between the initial abundances used in the models and the values observed in FG stars. The white line is a dilution curve, obtained by mixing different fractions of unprocessed material and gas from AGBs (see text for details). Right: same as left panel, but referred to the Na-N plane. The shift applied to the observed nitrogen abundances is -0.7 dex.

analysis focused on HB stars by Gratton et al. (2013), and by spectroscopy of unevolved stars of the same cluster (D’Orazi et al. 2010).

To understand whether this set of observations can be explained on the basis of the self-enrichment mechanism by AGBs, we compare the data available with the chemistry obtained by mixing gas from massive AGBs and SAGBs

with gas assumed to share the primeval chemistry of the cluster, characterizing the FG component.

The dilution of the chemistry reported in Table 1 for $M \geq 5M_{\odot}$ with pristine material defines an abundance pattern, for different degrees of dilution. Theoretically, all the results obtained with degrees of dilution ranging from 0 to 1 should be considered: however, the photometric analysis

of the HB (Di Criscienzo et al. 2010) and of the MS of 47 Tuc (Milone et al. 2012a) indicate that the range of helium abundances of the stars in the cluster is $\Delta Y \sim 0.03$, which rules out the possibility that uncontaminated stars with the pure chemistry of AGBs formed: based on the values shown in Table 1, these stars should have a helium mass fraction $Y \sim 0.35$, which would determine a much wider spread of the MS. These arguments allow to determine the minimum degree of dilution from which the stars in the SG formed: mixing of pristine matter with $Y = 0.26$ and gas from AGBs with $Y = 0.35$ leads to the maximum helium allowed from the photometric analysis, $Y = 0.29$, if we assume that the fraction of gas from AGBs used to form SG stars is one third, the remaining being provided by pristine gas in the cluster. In the following analysis we will allow the relative contribution from gas ejected by AGBs to range from a minimum of 0% to a maximum of 35%. Obviously stars formed with no AGB ejecta or with a very large fraction of pristine gas will have the chemical properties of FG stars and would not be classified as SG stars (D’Ercole et al. 2011).

Fig. 4 shows the results from Carretta et al. (2013) on the Na–Al (left panel) and Na–N (right) planes. In both axis we report the variation with respect to the abundances observed in the stars that we assume to belong to the first generation of the cluster. This choice is motivated by the offset between the solar-scaled abundances of nitrogen, aluminium and sodium used in our models, and the minimum values for the same elements reported in Carretta et al. (2013).

The AGB and SAGB yields reported in Table 1 are indicated with full, blue triangles. The white curve indicates a dilution relationship, obtained by mixing gas with the original chemistry of the cluster with matter ejected by AGBs; this analysis is particularly simple in this case owing to the little variation with mass of the chemistry of the ejecta in the massive AGBs domain, and would be harder to be applied to lower metallicity clusters, for which the composition of the ejecta is much more sensitive to the initial mass of the star. The dilution curves in Fig. 4 are limited in such a way that the contribution of AGB ejecta range from 0% to a maximum of 35%. As pointed out above, and previously discussed in D’Ercole et al. (2011), stars forming from a mix of gas with a large fraction of pristine gas would fall in the FG portion of the chemical patterns planes. We extend the lines to such a large fraction of pristine gas only for illustrative purposes.

We see from both panels that the observed trends, within the error bars associated to the abundances of the individual stars, are satisfactorily reproduced. In the Na–Al plane (left panel) most of the stars fall within the dilution curve, with the exception of two sources, that show a chemistry similar to the pure AGB ejecta. The same holds for the Na–N pattern, the dilution curve encompassing the most extreme, nitrogen-rich stars.

Fig. 5 shows the comparison between the theoretical predictions and the observations, for what concerns the oxygen–sodium anticorrelation. Similarly to the Na–Al and Na–N patterns showed in Fig. 4, we show the (negative) variation of the surface oxygen of the individual stars, assuming that the FG has an initial oxygen $[O/Fe] = +0.2$.

The comparison in this case is not straightforward, given the large uncertainties associated in particular to the abundances of oxygen. The abundances of the ejecta lay

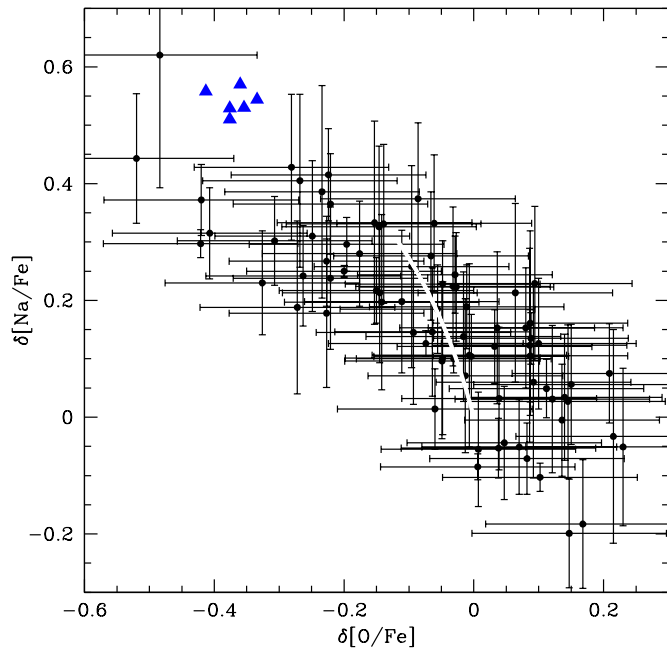


Figure 5. Same as Fig. 4, but referring to the O–Na plane. The sodium abundances observed were shifted as in Fig. 4. Because the initial oxygen in the models is $[O/Fe] = +0.2$, we applied a shift of -0.2 dex to the yields. The observed oxygen abundances were also shifted by -0.2 dex, to account for the difference between the initial oxygen in the models and the abundances observed in FG stars (see text for details).

in the upper-left portion of the plane, where the most contaminated objects are found. Given the arguments discussed previously, regarding the maximum degree of contamination by AGB gas in the formation of the second generation of stars, we must rule out such extreme chemistries, limiting the contribution from AGBs to 35%. In this way we obtain the dilution curve in Fig. 5. The observed points are reproduced within the error bars associated to the observations, with the exception of the three most extreme objects with the smallest abundances of oxygen. This comparison, though less meaningful than the previous analysis based on the abundances of aluminium and nitrogen, indicates that the HBB experienced by AGB models of the same chemistry as 47 Tuc stars is appropriate to provide the oxygen depletion needed to fit the observations.

A word of caution concerning the assumptions made on the chemical mixture from which the cluster formed (i.e. the composition of FG stars) is needed here. The results from the above analysis hold provided that the values used to build the models are correct, and that the observed data show an offset in the measured abundances. Should the initial aluminium be that observed in the assumed FG component (a factor of ~ 3 higher than our assumption), the magnesium nucleosynthesis would work with the same efficiency, thus the amount of Aluminium produced, $\delta(Al) = X(Al)_{\text{ejecta}} - X(Al)_{\text{initial}}$ would be unchanged: this would imply a smaller percentage increase in the content of Al in the ejecta, thus a smaller difference between the abundances of SG and FG stars. This can be easily compensated

by a higher content of magnesium, which we assumed to be $[\text{Mg}/\text{Fe}] = +0.2$, whereas data from Carretta et al. (2013) point in favour of a larger abundance of $[\text{Mg}/\text{Fe}] = +0.4$.

The situation is less critical for sodium, not only because the offset between our assumptions and the abundances given in Carretta et al. (2013) is limited to a factor ~ 2 , but also because the percentage increase in the surface sodium is only marginally touched by the initial abundance: the horizontal extension of the dilution curves in both panels of Fig. 4 would be slightly shorter, but the conclusion drawn would remain unchanged.

As far as oxygen is concerned, the rate of destruction of this species scales with its abundance, which makes the percentage reduction independent on the assumed initial value.

We do not discuss here the effects of a possible offset in the nitrogen content, because the absolute values are strongly interfaced with the assumptions concerning the initial carbon in the mixture, thus contain a high degree of arbitrariness. We limit our analysis on the variations observed.

According to the models used here, no change in the silicon abundance should be detected. This seems to be in agreement with the data from Carretta et al. (2013), where no clear Si–Al trend is observed.

Magnesium is only marginally touched by the HBB experienced, the decrease in the overall Mg being below 0.05 dex (see col. 11 of Table 1). The detection of a similar spread among 47 Tuc stars is behind the possibilities of the present observations, given the undetermination in the measured abundances, exceeding 0.1 dex (Carretta et al. 2013).

3.1 The faint turnoff in 47 Tuc

The analysis by Di Criscienzo et al. (2010) suggested the presence in 47 Tuc of a stellar component enriched in the overall C+N+O, based on the morphology of the SGB of the cluster. These faint turnoff stars should be revealed along the RGB. We suggest that they are the few stars in the left panel of Fig. 4 which are out of the dilution pattern but have high $[\text{Na}/\text{Fe}]$ and $[\text{Al}/\text{Fe}]$. The stars for which we have measures of oxygen have also low $[\text{O}/\text{Fe}]$, closer to the pure yields of our models.

Following the models by D’Ercole et al. (2012), we can think that the bulk of SG stars in 47 Tuc has been formed by dilution of pristine gas with the AGB ejecta. When the pristine gas gets consumed, the star formation may go on for a while, until type Ia supernovae completely clean the cluster from gas. The stars formed in this phase would have the chemistry of the $5M_{\odot}$ ejecta, scarcely diluted with pristine gas. The CNO enhancement of the $5M_{\odot}$ is 1.35 times the original CNO, and the turnoff location of these stars could resemble the faint turnoff. This small population should also be helium rich, so their HB location would be among the most brilliant HB stars of 47 Tuc.

Gratton et al. (2013) show indeed that a couple of their bright star groups of 47 Tuc HB also have high $[\text{Na}/\text{Fe}]$ and low $[\text{O}/\text{Fe}]$. The rest of their bright sample consists of normal FG stars, probably in an evolved phase out of the HB.

4 47 TUC: HOW THE MULTIPLE POPULATIONS FORMED

The analysis carried out in the previous section shows that dilution of massive AGBs ejecta with gas pristine allows to reproduce the observed patterns of 47 Tuc stars. This is in agreement with the scenario described by D’Ercole et al. (2008) and D’Ercole et al. (2010, 2011, 2012) according to which SG stars formed from a mix of AGB ejecta and pristine gas driven into the cluster central regions by a cooling flow and the SG formation process is halted after ~ 100 Myr by SN Ia explosions.

The chemistry with which SG stars form is therefore obtained by mixing processed matter with the chemical properties of the AGB and SAGB ejecta of stars evolving within ~ 100 Myr (i.e. for mass $M \geq 5M_{\odot}$, see col. 2 of Table 1) and pristine gas, with the same composition of FG stars. The presence of pristine gas is an essential ingredient in the self-enrichment mechanism by AGBs (as well as in all the other models proposed in the literature; see D’Ercole 2011 for a discussion), and allows to reproduce the O–Na anticorrelation, otherwise inhibited by the direct correlation between the oxygen and the sodium yields by massive AGBs (D’Ercole et al. 2011).

In the case of 47 Tuc, our models suggest that to reproduce the photometric and spectroscopic observations SG stars must have formed out of a mix of gas in which about one third came from the AGB and SAGB ejecta and the rest from pristine gas. According to Carretta et al. (2013) FG stars are $\sim 25\%$ of the total population, the remaining 75% being contaminated objects belonging to the SG. The fact that the gas ejected by massive AGBs, for any realistic mass function, is only $\sim 5\%$ of the mass of the initial FG population implies that a significant fraction of FG stars must have been lost by the cluster. According to the simulations presented in D’Ercole et al. (2008), this early loss of FG stars (and the consequent increase in the fraction of SG stars) would occur during the cluster early evolution. Memory of the initial central concentration of the SG population would be preserved during this phase and would still be present in many clusters today (Vesperini et al. 2013). Based on the analysis presented in Vesperini et al. (2013), 47 Tuc would be one of the clusters for which the SG should still be more concentrated in the inner regions than the FG population in agreement with what found in observational studies (Milone et al. 2012a; Richer et al. 2013).

Following the calculation presented in D’Antona et al. (2013) and applying it to the chemical model presented here in which SG stars formed from a mix composed AGB ejecta (one third) and pristine gas (two thirds), we estimate that the total initial FG mass of 47 Tuc was about 7.5 times the current cluster mass (assuming SG stars form with masses up to about $8M_{\odot}$ so that there are no SG SNII explosions (D’Antona et al. 2013); the initial mass required would be smaller—about 4.5 times the current cluster mass—if one assumes a range of SG stars limited to $0.8 M_{\odot}$).

5 CONCLUSIONS

In this paper we have studied the viability of a model to explain the abundance patterns defined by stars in 47 Tuc on the basis of the self-enrichment scenario by massive AGBs.

For this purpose, We have specifically calculated a full set of AGB and SAGB models with the chemistry of 47 Tuc stars, and iron content $[\text{Fe}/\text{H}] = -0.75$.

AGB models in the high mass ($M \geq 5M_{\odot}$) domain experience a soft Hot Bottom Burning, producing ejecta enriched in Aluminium and sodium by +0.5 dex, and depleted in their oxygen content by -0.4 dex. No meaningful magnesium and silicon variations are expected. Similarly to other metallicities, the matter ejected is helium-rich, $Y \sim 0.35$.

Mixing of gas ejected by AGBs with pristine gas sharing the same chemistry as the stars originally present in the cluster allows to trace abundance patterns, where sodium is correlated to nitrogen and aluminium, and anticorrelated to oxygen. Based on the maximum helium enhancement allowed by the photometric analysis of the HB and the MS of the same cluster, we estimate that SG stars formed from a mix of gas composed for about one third of AGB ejecta and two thirds of pristine gas. Using this constrain, we can fit the extension and the slopes of the various trends observed, provided that only stars with mass $M \geq 5M_{\odot}$ contributed to the formation of the second generation. This implies that the SG population formed formed within ~ 100 Myr, before the SN Ia explosions prevented further star formation.

Based on this analysis, and from the observed fraction of SG stars, $\sim 75\%$ of the total stellar population, we estimate that 47 Tuc was initially about 7.5 times more massive than now (or 4.5 times for SG star formation limited to $0.8 M_{\odot}$) and that a large fraction of its initial FG population must have been lost during the cluster early evolution.

ACKNOWLEDGMENTS

Funding is acknowledged PRIN INAF 2011 Multiple populations in GCs: their role in the Galaxy assembly (PI: E. Carretta), and PRIN MIUR 20102011 The Chemical and Dynamical Evolution of the Milky Way and Local Group Galaxies (PI: F. Matteucci), prot. 2010LY5N2T. EV was supported in part by grant NASA-NNX13AF45G. MDC has been supported by the INAF fellowship 2010 grant.

REFERENCES

- Anderson J., Piotto G., King I. R., Bedin L. R., Guhathakurta P., 2009, *ApJ*, 697, L58
- Bekki, K., Campbell, S. W., Lattanzio, J. C., & Norris, J. E. 2007, *MNRAS*, 377, 335
- Bekki, K. 2011, *MNRAS*, 412, 2241
- Blöcker T., Schönberner D., 1991, *A&A*, 244, L43
- Briley M., 1997, *AJ*, 114, 1051
- Caloi V., D’Antona F., 2005, *A&A*, 435, 987
- Caloi V., D’Antona F., 2007, *A&A*, 463, 949
- Cannon R. D., Croke B. F. W., Bell R. A., Hesser J. E., Stathakis R. A., 1998, *MNRAS*, 298, 601
- Canuto V. M. C., Mazzitelli I., 1991, *ApJ*, 370, 295
- Carretta E., Gratton R. G., Bragaglia A., Bonifacio P., Pasquini L., 2004, *A&A*, 416, 925
- Carretta E., Bragaglia A., Gratton R., et al., 2009, *A&A*, 505, 117
- Carretta E., Gratton R., Bragaglia A., D’Orazi V., Lucatello S., 2013, *A&A*, 550, A34
- Cloutmann L., & EoLL J.G., 1976, *ApJ*, 206, 548
- D’Antona F., Bellazzini M., Caloi V., Fusi Pecci F., Galletti S., Rood R. T., 2005, *ApJ*, 631, 868
- D’Antona F., Caloi V., Montalbán J., Ventura P., Gratton R., 2002, *A&A*, 395, 69
- D’Antona F., Caloi V., 2004, *A&A*, *ApJ*, 871
- D’Antona F., Caloi V., D’Ercole A., Tailo M., Vesperini E., Ventura P., Di Criscienzo M., 2013, *MNRAS*, 434, 1138
- Decressin, T., Charbonnel, C., & Meynet, G. 2007, *A&A*, 475, 859
- de Mink, S. E., Pols, O. R., Langer, N., & Izzard, R. G. 2009, *A&A*, 507, L1
- D’Ercole A., Vesperini E., D’Antona F., Mc Millan S. L. W., Recchi S., 2008, *MNRAS*, 391, 825
- D’Ercole A., D’Antona F., Ventura P., Vesperini E., Mc Millan S. L. W., 2010, *MNRAS*, 407, 854
- D’Ercole A., D’Antona, F., Vesperini E., 2011, *MNRAS*, 415, 1304
- D’Ercole A., D’Antona F., Carini R., Vesperini E., Ventura P., 2012, *MNRAS*, 423, 1521
- D’Orazi V., Lucatello S., Gratton R., Bragaglia A., Carretta E., Shen Z., Zaggia S., 2010, *ApJ*, 71, L1
- Di Criscienzo M., Ventura P., D’Antona F., Milone A., Piotto G., 2010, *MNRAS*, 408, 999
- Garcia Berro E., Ritossa C., Iben I. J., 1997, *ApJ*, 485, 765
- Gratton R., Sneden C., Carretta E., 2004, *AR&A*, 42, 385
- Gratton R., Carretta E., Bragaglia A., 2012, *AR&Av*, 20, 50
- Gratton R.G., Lucatello S., Sollima A., Carretta E., Bragaglia A., Momany Y., D’Orazi V., Cassisi S., Pietrinferni A., Salaris, M., 2013, *A&A*, 549, 41
- Grevesse N., Sauval A. J., 1998, *SSrv*, 85, 161
- Harbeck, D., Smith G. H., Grebel E. K., 2003, *AJ*, 125, 197
- Herwig F., 2005, *AR&A*, 43, 435
- Karakas A. I., 2010, *MNRAS*, 403, 1413
- Karakas A.I. 2011, in "Why Galaxies Care about AGB Stars II: Shining Examples and Common Inhabitants" ed. F. Kerschbaum, T. Lebzelter, and R.F. Wing. San Francisco: Astronomical Society of the Pacific, 2011., p.3
- Marigo P., Girardi L., 2007, *A&A*, 469, 239
- Marino, A. F., Villanova, S., Piotto, G., et al. 2008, *A&A*, 490, 625
- Marino, A. F., Milone, A. P., Piotto, G., et al., 2009, *A&A*, 505, 1099
- Milone A. P., Bedin L. R., Piotto G., et al., 2008, *ApJ*, 673, 241
- Milone A. P., Piotto G., King, I. R., Bedin L. R., Anderson J., Marino A. F., Momany Y., Malavolta L., Villanova S., 2010, *ApJ*, 709, 1183
- Milone, A.P., Piotto G., Bedin L. R., et al., 2012a, *ApJ*, 744, 58
- Milone, A. P., Marino, A. F., Piotto, G., et al. 2012b, *ApJ*, 745, 27
- Milone, A. P., Marino, A. F., Piotto, G., et al. 2013, *ApJ*, 767, 120
- Nataf D. M, Gould A., Pinsonneault M. H., Stetson P. B., 2011, *ApJ*, 736, 94
- Norris J. E., Freeman K. C., Mighell K. J., 1996, *ApJ*, 462, 241
- Piotto G., Bedin L. R., Anderson J., et al., 2007, *ApJ*, 661,

L53

- Piotto G., Milone A. P., Anderson J., et al., 2012, *ApJ*, 760, 39
- Renzini, A. 2008, *MNRAS*, 391, 354
- Renzini A., Voli M., 1981, *A&A*, 94, 175
- Renzini, A. 2013, *Mem. Soc. Astron. Italiana*, 84, 162
- Richer H. B., Heyl J., Anderson J., Kalirai J. S., Shara M. M., Dotter A., Fahlman G. G., Rich M., 2013, *ApJL*, 771, L15
- Ritossa C., Garcia Berro E., Iben I. J., 1996, *ApJ*, 460, 489
- Ritossa C., Garcia Berro E., Iben I. J., 1999, *ApJ*, 515, 381
- Schwarzschild M., Harm R., 1965, *ApJ*, 142, 855
- Schwarzschild M., Harm R., 1967, *ApJ*, 145, 496
- Siess L., 2006, *A&A*, 448, 717
- Siess L., 2007, *A&A*, 476, 893
- Siess L., 2010, *A&A*, 512, A10
- Ventura P., Carini R., D'Antona F., 2011, *MNRAS*, 415, 3865
- Ventura P., D'Antona F., 2005, *A&A*, 341, 279
- Ventura P., D'Antona F., 2006, *A&A*, 457, 995
- Ventura P., D'Antona F., 2008a, *A&A*, 385, 2034
- Ventura P., D'Antona F., 2008b, *A&A*, 805, 816
- Ventura P., in *Proceedings of the IAU Symposium No. 268, Light Elements in the Universe*, ed. C. Charbonnel, M. Tosi, F. Primas & C. Chiappini, 2009
- Ventura P., D'Antona F., 2009, *A&A*, 499, 835
- Ventura P., D'Antona F., 2011, *MNRAS*, 410, 2760
- Ventura P., D'Antona F., Mazzitelli I., Gratton, R., 2001, *ApJ*, 550, L65
- Ventura P., Di Criscienzo M., Carini R., D'Antona F., 2013, *MNRAS*, 431, 3642
- Ventura P., Zeppieri A., Mazzitelli I., D'Antona F., 1998, *A&A*, 334, 953
- Vesperini E., McMillan S. L. W., D'Antona F., D'Ercole A., 2013, *MNRAS*, 429, 1913